JOURNAL OF CATALYSIS 59, 211–222 (1979)

Characterization and Performance of Platinum–Iridium Reforming Catalysts

J. C. RASSER,[1] W. H. BEINDORFF, AND J. J. F. SCHOLTEN[2]

Laboratory for Chemical Technology, Delft Technical University, Julianalaan 136, 2628 BG Delft, The Netherlands

Received September 15, 1978; revised December 11, 1978

In view of the limited insight into the factors which play a part in the improving action of iridium in reforming with platinum–iridium-on-γ-alumina as a catalyst, a study is made of the texture and composition of a number of catalysts with varying Ir/Pt ratios. Using Auger electron spectroscopy an analysis is made of the surface composition of a number of platinum–iridium alloy powders, before and after contact with propane. *n*-Heptane and *n*-hexane reforming is studied as a model reaction, and the influence of the Ir/Pt ratio on the isomerization, cyclization, and aromatization selectivities is determined. In the alloy powders a strong platinum surface enrichment is found, in accordance with the platinum-like behavior of the catalysts. The main function of iridium appears to be the suppression of surface carbiding.

INTRODUCTION

Among the numerous bi- and multimetallic reforming catalysts, applied or proposed since the discovery of the Pt/Re-on-γ-alumina catalyst (*1*), Pt/Ir-on-γ-alumina (*2–6*) seems to occupy a special place. Just as with the Pt/Re and Pt/Ge systems, addition of the second component (Ir) leads to an improvement of the octane number (more branched alkanes, cycloalkanes, and aromatics) and a lowering of the rate of coke deposition, resulting in an increased stability. As compared with the metals in the Pt/Re and Pt/Ge system, platinum and iridium show a greater physical and chemical similarity. Therefore, an explanation of the beneficial action of iridium in terms of a ligand or an ensemble effect (*7*) seems, at first sight at least, quite difficult.

Some physical–chemical data of platinum and iridium, neighbors in group VIII of the periodic table, are summarized in Table 1. A striking difference exists between the melting points, the heats of evaporation, and the surface tensions, pointing to the metal–metal bond in iridium being much stronger than in platinum.

A limited mutual solubility of the metals is reported (*8*), and we may ask ourselves if in the bimetallic catalysts alloy particles are formed. The phase diagram shows a broad miscibility gap with a critical point at 1284 K at the 50/50 composition. At 970 K the iridium-poor phase contains about 7 atom% Ir, and the Ir-rich phase about 1 atom% Pt. However, the two phases crystallize out extremely slowly (*8*), and the alloys initially solidify without

---

[1] Present address: Procter and Gamble European Technical Centre, Strombeek near Brussels, Belgium.

[2] To whom all correspondence should be directed.

0021-9517/79/110211-12$02.00/0

TABLE 1

Physical–Chemical Properties of Platinum and Iridium

	Platinum	Iridium	Reference
Type of lattice	f.c.c.	f.c.c.	(*8*)
Lattice constant	0.3916 nm	0.3831 nm	(*8*)
Electron work function	5.27 eV	5.40 eV	(*9*)
Melting point	2042 K	2716 K	(*10*)
Heat of evaporation	565.3 kJ/mole	665.3 kJ/mole	(*10*)
Surface tension[a]	1865 J/m^2	2250 J/m^2	(*11*)

[a] For polycrystalline material near the melting point.

phase separation, as follows from crystallographic observation (*8*). Furthermore, highly dispersed alloys on carriers have thermodynamic properties deviating from nondispersed systems, and various methods of *chemical* alloy formation in catalyst preparation may lead to perfect solid solutions (see the Experimental section).

Catalytic Behavior of Platinum–Iridium Alloys

To promote intimate mixing and cluster formation, the catalysts are mostly prepared by simultaneous impregnation of γ- or η-alumina with aqueous solutions of chloroplatinic and chloroiridic acid, and, after drying, calcining in air at 533 to 643 K (*2–6*). As the reforming catalysts are dual-functional (*12, 13*), addition of chlorine is essential to make the surface of the support acidic.

Very little is published about the fundamentals of the reforming behavior. In the patents (*2–6*) a wide composition range is claimed, with a certain preference for the fifty–fifty composition. Whereas the pure platinum catalysts are outstanding for the selective conversion of naphthenes to aromatics, but limited in their ability to convert paraffinic components in the feed, the Pt/Ir catalysts have a high isomerization and dehydrocyclization activity for paraffins, besides a higher yield stability. However, according to Anderson and Avery (*9*), pure iridium has *no* isomerization activity and is more active for hydrocracking.

Ramaswamy *et al.* (*14*) report an improved yield of isomerization products on adding sulfur. The sintering resistance of their catalyst, 10 Ir/90 Pt-on-γ-alumina, was not superior to that of the monometallic one. The superior performance of the catalyst is ascribed to the dilution of Pt by Ir, which should have a lower concentration of coke precursors on its surface.

In the conversion of heptane over α-alumina-supported Pt/Ir catalysts, Tournayan *et al.* (*15*) report a platinum-like behavior for Ir/Pt ratios up to 2.3.

A number of authors have claimed a relationship between catalytic activity and the d-band structure of platinum–iridium catalysts. Gray *et al.* (*16*), studying the conversion of pentane to isopentane, arrived at an increased rate at the composition 25 Ir/75 Pt, only 1.15 times higher than found for pure platinum. Bond and Webster (*17, 18*) studied the reduction of nitrobenzene dissolved in methanol over Pt/Ir at 303 K, and reported an activity maximum around 15 to 20 atom% Ir. There was, however, great uncertainty about the actual state of the catalysts in their work (alloys or mixed oxides), and no firm conclusion was possible. Kroptova and co-workers (*19*) studied the electrocatalytic reduction of acetone in 1 *N* sulfuric acid over Pt/Ir Raney catalysts (solid solutions at all compositions). The apparent activation energy was found to be a factor 4 to 5 lower just at the composition 25 atom% Ir/75 atom% Pt. In this work, sulfuric acid may have strongly influenced the surface composition of the alloy.

We conclude that there is no clear evidence from the literature for the existence of a special ligand effect (or, in terms of the band model, an influence of the electronic structure) at a certain preferred Pt/Ir ratio.

Thermodynamics of the Platinum–Iridium System

Ramakrishnan and Chandrasekharaiah (RC) (*20*) calculated the free enthalpy of mixing for different alloy compositions from measurements of the thermodynamic activity of Ir in Pt/Ir alloys, using the volatility of IrO_3 at 1468 and 1518 K as a measure of the activity of Ir. In the composition range Pt_3Ir the integral molar free energy of mixing shows a maximum of 6.19 kJ/mole.

We make the following critical remarks:

RC's results are inconsistent with those of Raub and Plate (*8*), where *no* maximum in the composition range Pt_3Ir is found.

Enrichment of the alloy surfaces with platinum, and iridium surface depletion by oxygen, may have strongly disturbed RC's measurements.

Due to the large difference in the temperature of alloy preparation and the temperature at which the IrO_3 volatility was measured (ΔT was about 1000 K), there was no equilibrium between the surface and bulk composition. Nevertheless, in RC's work the Ir activity was related to the surface composition.

But even if we accept RC's results, we should be aware that the maximum found by them in the platinum–iridium interaction energy at the composition Pt_3Ir (of 6.19 kJ/mole) is only of the order of a weak physical interaction, and a factor of about 10^2 smaller than the Pt–Pt and Ir–Ir binding strength.

We conclude that there is no clear evidence from the thermodynamics of the system for the existence of an ordered Pt_3Ir phase.

Scope of the Present Work

In view of the limited insight into the factors which play a part in the improvement of reforming by adding iridium to Pt-on-γ-alumina catalysts, we decided to make a closer study of this bimetallic system. An Auger electron spectroscopy (AES) study of the surface composition of alloy powders was undertaken in a wide composition range. Furthermore, the selectivity in hydroreforming, with hexane and heptane as model compounds, was investigated.

EXPERIMENTAL

Alloy powders. Pt, Ir, and Pt/Ir alloy powders were prepared by reduction of aqueous solutions of H_2PtCl_6, H_2IrCl_6, or mixtures thereof, reagent grade, by adding these solutions to a boiling solution of hydrazine, according to the method of Kulifay (*21*).

From X-ray diffraction it appeared that all the powders were monophasic solid solutions, their lattice constants corresponding to the geometric mean value, calculated from the composition and from the lattice constants of Ir and Pt, as given by Raub and Plate (*8*).

From X-ray line broadening the weight-mean diameter $\bar{d}_w$ was found. The surface area $S(\bar{d}_w)$ was calculated from $\bar{d}_w$, with $S(\bar{d}_w) = 6V/\bar{d}_w$. This equation is valid for nearly spherical particles. V is the specific volume of the metal. BET surface areas, calculated from the physical adsorption isotherms of methane at 77 K, are presented in Table 2.

AES spectra were recorded with an Auger electron spectrometer from Physical Electronics Inc.[3] Before measuring the spectra, thin pressed pellets of the powders were reduced overnight in a flow of ultra

---

[3] These measurements were carried out in cooperation with Dr. F. J. Kuijers, Department of Heterogeneous Catalysis, Gorlaeus Laboratory, University of Leiden.

TABLE 2

Weight Mean Diameters and Surface Areas of Kulifay Metal Powders

	$\bar{d}_w$ (nm)	$S(\bar{d}_w)$ (m^2/g)	S(BET) (m^2/g)
Pt	26	10.7	11.1
Ir	30	8.8	9.8
50% Pt/50% Ir	29	9.3	9.6

pure hydrogen at 673 K. Next they were brought into the Auger vacuum chamber, which was evacuated down to a pressure of 10^{-8} Torr in a few hours. Evacuation was followed by cleaning by means of an argon ion bombardment (energy 2.5 keV), at 10^{-5} Torr (1 Torr = 133.3 N m^{-2}). Before measuring the spectra the pellets were sintered overnight at 673 K.

Supported catalysts. In most experiments γ-alumina (from Akzo, Amsterdam, type 003P, S(BET) = 248 m^2/g) was used as a support. For some experiments α-alumina, from Rhône Progil, France, type SCS9, S(BET) = 24 m^2/g, was chosen. About 5 g of the support was stirred into 30 ml of water, and 4 ml of concentrated HCl (37 wt% HCl in water) was added, in order to increase the surface acidity of the support. Next, a solution containing the required amounts of H_2PtCl_6 and/or H_2IrCl_6 was added dropwise.

After 1 hr of stirring the thick paste was dried in a porcelain crucible at 360 K for 16 hr, followed by calcining in air at 820 to 870 K for 16 to 20 hr, and reduction in hydrogen at 650 K for 8 hr.

A number of samples on γ-alumina were investigated by X-ray diffraction; in all cases monophasic alloy particles were found. Line broadening revealed that the mean particle size was relatively high as compared to what is normally found in reforming catalysts (Table 3). For instance, Ramaswamy *et al.* (*14*) report a mean diameter of only 1.7 nm for their Pt/Ir-on-γ-alumina sample. The higher values found in this work are due to the relatively high temperature of calcination.

The iridium and platinum contents of the catalysts were calculated from the amounts weighed in, and controlled by means of activation analysis (*22*).

Other chemicals. Hydrogen was purified by diffusion through a Pd thimble. Helium was led over a copper-on-alumina catalyst (type R3-11, from BASF, Germany), and dried over molecular sieves type 3A, from Linde, U.S.A. Hexane and heptane were from Merck, Germany, "für die Spektroskopie."

Apparatus and procedure. Hydrocarbon conversion reactions were carried out in an apparatus shown schematically in Fig. 1. A constant flow of H_2, purified as indicated above, and metered by means of a Porter precision flow controller, type VCD-1000, was passed through an evaporator, where it was saturated with the hydrocarbon vapor to be converted. In the condenser the gas mixture was cooled to a prechosen temperature so as to achieve a hydrogen–hydrocarbon ratio of about 17. The reactor consisted of a U-shaped stainless-steel tube, 4 mm in diameter, in which the position of the catalyst was fixed by means of quartz wool. A uniform reactor temperature was obtained by making use of a fluid bed oven, filled with fine silica particles. The temperature remained constant within 1 K, and the uniformity of the temperature over the length of the bed was better than 0.1 K.

At regular time intervals the product stream was analyzed by means of gas/liquid chromatography. The column was a 3 m silanized stainless-steel tube of 3-mm internal diameter, filled with 25% squalane on Chromosorb WAW (100–120 mesh). The column was thermostated at 325 ± 0.5 K. The flow of the carrier gas (He) was maintained at 0.76 ml (NTP)/sec. Toluene had the longest retention time (4700 sec), so that total analysis took about 1.5 hr. By way of example, in the hydroreforming of heptane over a Pt/Ir-on-γ-alumina catalysts at 650 K, the following products were analyzed:

Hydrogenolysis products: methane, ethane, propane, butane, methylbutane, pentane, 2-methylpentane, 3-methylpentane, hexane.

Skeletal isomerization products: 2,2-dimethylpentane, 2,4-dimethylpentane, 2,3-dimethylpentane, 3-methylhexane, 3-ethylpentane, 2-methylhexane.

Cyclization products: methylcyclohexane, ethylcyclopentane.

Aromatization product: toluene.

The following reaction conditions were maintained: temperature in the reactor, 650 ± 1 K; pressure, 10^5 N m^{-2}; H_2/hexane or H_2/heptane ratio, 18; flow, 100 mm^3 sec^{-1}. Amount of catalyst: 2 g in the hexane experiments, and 0.5 g in the heptane experiments.

Instead of reporting all conversion products detected, we present the following selectivities (for the case of heptane conversion):

S_h = the hydrogenolysis or hydrocracking selectivity

$$= \frac{\text{total of hydrocarbons with less than 7 C-atoms}}{\text{total of converted heptane}} \times 100$$

$$S_i = \text{skeletal isomerization activity} = \frac{\text{total of branched alkanes with 7 C-atoms}}{\text{total of converted heptane}} \times 100$$

$$S_c = \text{cyclization selectivity} = \frac{\text{all cyclic hydrocarbons, aromatics excluded}}{\text{total of converted heptane}} \times 100$$

$$S_a = \text{aromatization selectivity} = \frac{\text{total of aromatics}}{\text{total of converted heptane}} \times 100$$

$$\text{The conversion is given by: } \frac{\text{number of moles converted}}{\text{number of moles in the feed}} \times 100.$$

In the above definitions, "7 C-atoms" should be replaced by "6-atoms," and "heptane" by "hexane," when hexane conversion is discussed.

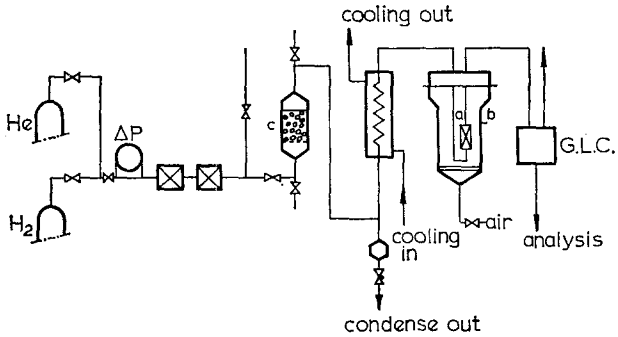

FIG. 1. Apparatus for hydrocarbon conversion. (a) reactor; (b) fluid bed oven; (c) heptane or hexane evaporator.

TABLE 3

Mean Particle Size of Alloy Particles in Pt/Ir-on-γ-Alumina Catalysts, from X-Ray Line Broadening

Sample number	Metal load (wt%)	Atomic ratio Ir/Pt	$\bar{d}_w$ (nm)
W 13	1.70	0	86
W 12	1.68	0.003	35
W 14	1.67	0.006	52
W 30	1.42	0.015	64
W 22	1.18	0.036	49
W 29	0.41	0.34	[a]
W 26	0.28	0.67	[a]

[a] Due to the low metal content the mean particle size could not be detected.

RESULTS

Auger Spectra of Platinum–Iridium Powders

The AES peaks of platinum and iridium in the 50 to 60 eV range correspond with an escape depth of about 0.5 nm (about two atomic layers), and hence their intensities are suited for measurement of the surface composition. Peaks in the 2000 eV range can be used in determining the bulk composition, the escape depth being here about 20 nm, which corresponds to about 10 monolayers (*23*). Results for Kulifay powders are given in Table 4 and plotted in Fig. 2. Since platinum and iridium are neighbors in the periodic table, we assume the back scattering factors to be the same for both metals. Corrections are made for the difference in Auger electron yield.

Notwithstanding the high purity of the starting materials used in the preparation of the alloy powders, Auger peaks of carbon, sulfur, and oxygen, corresponding with surface concentrations more than 5% of full coverage were detected, and this hampered the precision of the determination of the Pt/Ir surface ratio.

Figure 2 shows that a platinum surface enrichment is found for most samples, in accordance with the rule (*7*) that the component with the lowest surface tension should accumulate at the surface (compare

TABLE 4

Bulk and Surface Composition of Pt/Ir Kulifay Powders

Sample number	Bulk composition (as weighed in) atom% Pt	Bulk composition (from Auger analysis[a]) atom% Pt	Surface composition (from Auger analysis[b]) atom% Pt
1	12	11	5[c]
2	16	15–19	6–9[c]
3	50	54	66
4	50	50–51	70
5	50	63–64	90–93

[a] Based on the intensity of the Pt peak at 2044 eV, and of the Ir peak at 1908 eV. Escape depth about 10 atomic surface layers.

[b] Based on the intensity of the Pt peak at 64 eV and of the Ir peak at 54 eV. Escape depth about two atomic surface layers.

[c] Repeated hydrogen treatment did not influence these results.

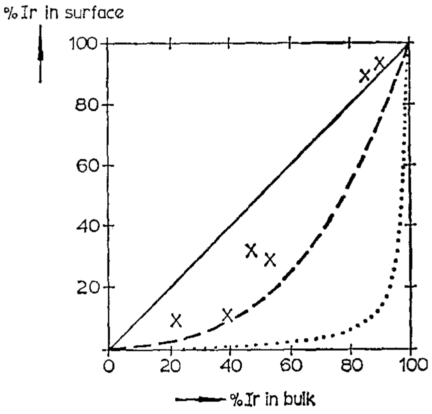

FIG. 2. Surface composition versus bulk composition of Kulifay powders, as determined by AES. Solid line: surface composition equal to bulk composition. Crosses: experimental points for Kulifay powders. Molar ratios of intensities, corrected for different elemental sensitivity, for surface- and bulk-sensitive peaks. Dashed line: experimental curve for equilibrated platinum–iridium alloy films. The same magnitudes are plotted here as with the crosses. Dotted line: calculated composition of the outermost layer of the alloy films.

surface tensions in Table 1). The surfaces of the two samples richest in iridium (see Fig. 2) were slightly surface-enriched in Ir; we think this is an artefact caused by the method of preparation.

Kuijers (*23*), in an Auger study of equilibrated platinum–iridium alloy films, found a somewhat stronger surface platinum enrichment for all Pt/Ir ratios (dashed line in Fig. 2). Applying Gallon's model for the Auger intensities (*24*), Kuijers also calculated the composition of the outermost layer (dotted line in Fig. 2).

With the 50 atom% Ir-containing sample 4 (Table 4), the rate of carbon deposition was studied by admitting propane at 300 K to the AES vacuum chamber, which was still connected with the vac-ion pumps, so that a steady-state partial pressure of 6×10^{-8} Torr was built up. The 280 eV carbon peak showed a considerable growth with time, indicating that some kind of carbon-containing deposit is formed on the surface. Simultaneously the intensities of the low-energy iridium and platinum peaks dropped markedly, but the rate of this process was higher for the relative platinum signal than for the relative iridium signal (Fig. 3).

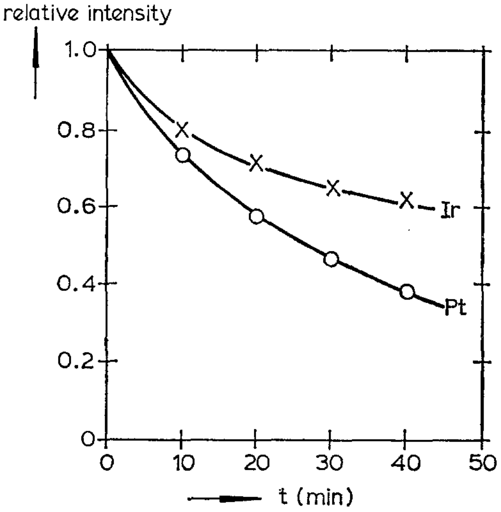

FIG. 3. Decline of the relative iridium and platinum Auger peak intensities as a function of time, upon exposure to propane at 300 K. Kulifay Pt/Ir with 50 atom% Ir in the bulk.

The decrease of the relative intensities proceeded to values of 0.63 (Ir) and 0.40 (Pt). Obviously a monolayer of a carbon-containing compound is formed gradually, which masks the Auger signals of surface platinum and iridium atoms to about half their original values. The slower and less extensive coverage of iridium as compared with platinum must be due to the higher activity of the iridium for the hydrogenolysis of propane to methane.

Pure iridium powder and the alloy powders No. 1 and 2 (Table 4) all carbided up to a coverage of at least one monolayer of carbon (as appeared from the total disappearance of the platinum and iridium Auger signals in the 50–60 eV range), were heated overnight in 10^{-6} Torr hydrogen at 673 K. This resulted in a weakening of the carbon Auger signal intensities to less than 5% of their original values. With platinum powder and with samples No. 3, 4, and 5, all relatively rich in platinum, the remaining signals were *appreciably* higher after the same treatment. Hence, once a carbonaceous deposit is formed, iridium and iridium-rich surfaces are much more easily freed from carbon by hydrogen. It follows from the foregoing that Brunelle, Montarnal, and Sugier's conclusion (*25*) that iridium has a higher hydrogenolytic activity than platinum, may be extended to iridium-rich platinum alloys.

That iridium shows a weaker tendency than platinum to form carbonaceous graphite-like deposits on its surface, and is more easily decarbided by hydrogen, might be related to the fact that the individual carbon atoms are more strongly bound to the iridium surface. The better located and more tightly bound carbon atoms are less suited for the formation of carbon–carbon bonds between chemisorbed carbon atoms, and the absence of these bonds would make these atoms more

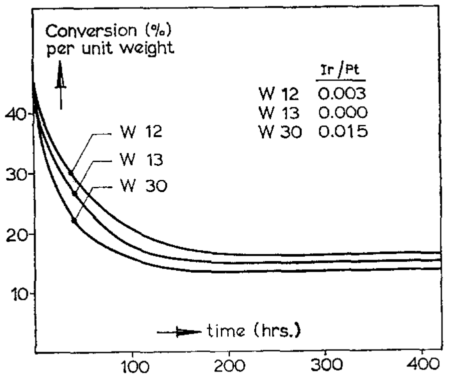

FIG. 4. Heptane conversion per unit metal weight, as a function of time. Iridium-poor catalysts.

active for hydrogenation to methane. The following facts support this view:

The heat of dissociation of gaseous IrC is slightly higher than of gaseous PtC, viz. 621 against 608 kJ/mole for PtC (*26*, *27*).

The bonding between iridium atoms is stronger than between platinum atoms (see the heats of evaporation, Table 1). Hence we might expect the chemisorption bond between carbon atoms and the iridium surface to be stronger than the corresponding bond between carbon atoms and the platinum surface.

Conversion of Hexane and Heptane over Alumina-Supported Platinum–Iridium Catalysts

In order to arrive at a better understanding of the promoting action of iridium, reforming of *n*-hexane and of *n*-heptane was studied as a model reaction. It has to be emphasized that our experiments were performed at a much lower pressure (10^5 N m^{-2}) and temperature (650 K) than is usual in industrial practice. Furthermore, the mean diameters of the metal crystallites were about 50 times as high as in industrial catalysts (Table 3). This has the advantage that the surface composition of these crystallites may be compared with that of the Kulifay powders discussed in the foregoing section. [Notice that the surface enrichment rules may change for very small crystallites (7)].

a. Running in the catalysts. In Figs. 4 and 5, the change of heptane conversion as a function of the running-in time is presented for seven samples with increasing iridium–platinum ratio.

First the samples were subjected to *in situ* reduction in a hydrogen flow of 100 mm^3 (NTP)/sec, at 650 K for 16 hr. Subsequently, the hydrogen–heptane mixture was fed to the reactor, which was at 650 K.

With six catalysts, all with an Ir/Pt ratio below 0.02, a slow but prolonged deactivation as a function of time was observed. By way of example, this general behavior is shown in Fig. 4 for catalysts W 12, W 13, and W 30.

During deactivation the material balance over the reactor showed a hydrocarbon deficit, indicating that some kind of carbonaceous deposit is formed on the catalyst surface. Indeed, after use, these iridium-poor catalysts had a dark-grey color, and after heating in air for 1 hr at 770 K, the weight loss was about 5%. The pure platinum catalyst W 13 showed a loss on ignition of even 10%.

Catalysts with Ir/Pt ratios > 0.02 had somewhat lower initial conversions (Fig. 5). For unknown reasons these conversions

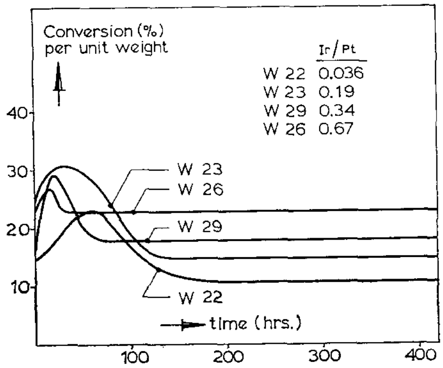

FIG. 5. Heptane conversion per unit metal weight, as a function of time. Iridium-rich catalysts.

first pass through a maximum and then decrease again, after which constant steady-state conversions are reached. The higher the Ir/Pt ratio, the lower the maximum and the shorter the time to reach the steady state. The final steady-state conversions increase with increasing Ir/Pt ratio, and surpass the steady-state activities of platinum and iridium-poor platinum catalysts.

It is important to note that all catalysts with an Ir/Pt ratio above 0.02 showed little carbon deposition; their loss on ignition was less than 1 wt%, and used catalysts were only slightly darker in color than the fresh ones.

Selectivity changes during the running-in period were also detected. The behavior of catalyst W 22 (Fig. 6) is typical for iridium-poor catalysts, platinum included. S_a and S_c increase at the cost of S_i, and the selectivities reach constant steady-state values after about 140 hr.

Catalysts with high Ir/Pt ratios attained their steady-state selectivity values already after 10 hr (see Fig. 7; catalyst W 29 with Ir/Pt = 0.34). The final steady-state selectivities S_i, S_c, and S_a were about equal to those found for platinum and the iridium-poor platinum catalysts (compare Figs. 6 and 7).

b. Conversion and selectivity in the steady state. The steady-state heptane conversions per unit metal weight (reached after a running-in period of 200 hr) are plotted in Fig. 8 as a function of the Ir/Pt ratio.

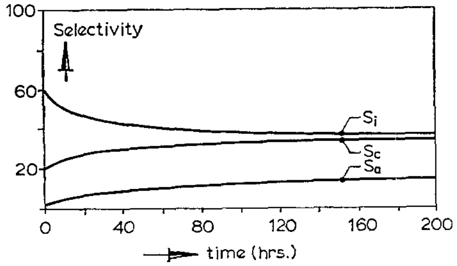

FIG. 6. Heptane reforming during the running-in period. The change of cyclization (S_c), isomerization (S_i), and aromatization (S_a) selectivities, as a function of time. Iridium-poor catalyst W 22 (Ir/Pt = 0.036).

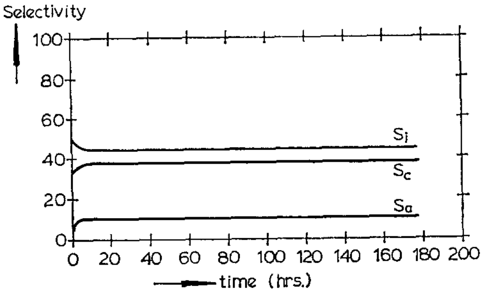

FIG. 7. Heptane reforming during the running-in period. The change of cyclization (S_c), isomerization (S_i), and aromatization (S_a) selectivities, as a function of time. Iridium-rich catalyst W 29 (Ir/Pt = 0.34).

For 10 catalysts with Ir/Pt ratios below 0.02, the steady-state conversions fluctuated between 6 and 10%, but for catalysts with Ir/Pt > 0.02, constant and reproducible conversions were arrived at. These conversions were a factor of about two higher than found for the iridium-poor catalysts, in accordance with their lower degree of carbon deposition (see Fig. 8).

Some very important observations are plotted in Fig. 9. For all catalysts with Ir/Pt ratios between 0.06 and 1.35, the

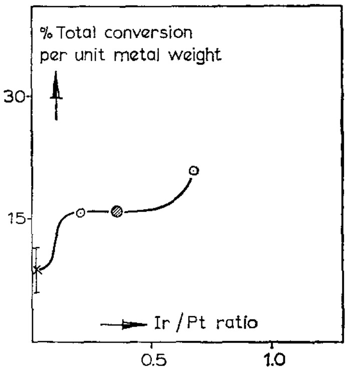

FIG. 8. Heptane conversion per unit metal weight, as a function of the Ir/Pt ratio, *in the steady state.* X, mean value for ten catalysts with Ir/Pt ratios below 0.02. The observed minimum and maximum conversions are indicated; ⊘, O, iridium-rich catalysts; ⊘, with a new batch this result reproduced within 2%.

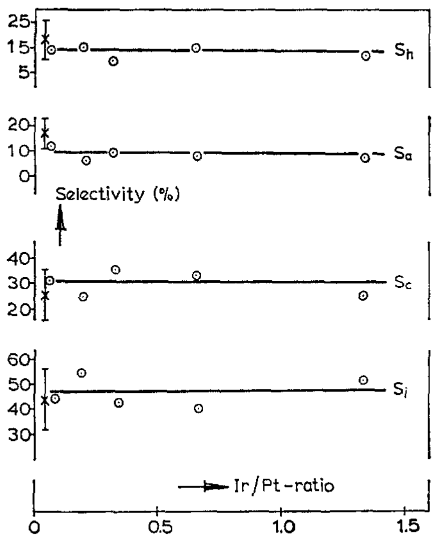

FIG. 9. Selectivities *in the steady state* as a function of the Ir/Pt ratio. X, mean value for 10 catalysts with Ir/Pt ratios below 0.02. The observed minimum and maximum selectivities are indicated.

steady-state selectivities S_h, S_a, S_c, and S_i are independent of the Ir/Pt ratio, and their values do not differ very much from the values found for platinum and iridium-poor platinum (the crosses in Fig. 9).

c. The bifunctional character of the process. An acidified γ-alumina catalyst (prepared in the same way as all the other catalysts, but without adding platinum and iridium) showed, under the conditions mentioned in the Experimental section, no hexane or heptane cracking or reforming activity. We also performed a number of experiments with iridium–platinum on α-alumina as a support. This type of alumina is inert and nonacidic, and hence the results (Table 5) are representative for the behavior of unsupported catalysts. Only hydrogenolysis (methane formation) was observed. The conditions were nondifferential, but Tournayan *et al.* (*15*), measuring heptane conversion over α-alumina-supported iridium under differential conditions, report similar results, their hydrogenolysis activity being about 90%.

As distinct from the behavior of nonsupported iridium (*14–16*) and of iridium on α-alumina, where only hydrogenolysis is observed, heptane conversion over 0.24% Ir-*on-acidified-γ-alumina* gave skeletal isomerization (selectivity 70%) and hydrogenolysis (selectivity 30%).

The above results demonstrate that neither the acidic sites nor the metal sites alone govern the reforming behavior of our catalysts. Hence, just as was demonstrated by Weisz (*28*) in his classical study of reforming with platinum on acidic supports, we are dealing here with bifunctional catalysis, in which an alkane is first dehydrogenated on a metal site, next isomerized on an acidic site, and finally hydrogenated on the metallic part of the surface.

DISCUSSION

In bimetallic reforming catalysts, such as Pt/Sn, Pt/Al, and Pt/Ge on γ-alumina, platinum is diluted with an inert second metal. The function of this second metal is mainly to isolate the surface platinum atoms rather than to change the activity per atom. This dilution results on the

TABLE 5

Hexane Conversion over α-Alumina-Supported Platinum–Iridium Catalysts

Catalyst	Metal load (wt%)	Ir/Pt ratio	Conversion (%)	S_i (%)	S_c (%)	S_a (%)	S_{methane} (%)
W6	5.6	32/68	100	0	0	0	100
W5	12.8	70/30	100	0	0	0	100
W10	5.8	100/0	100	0	0	0	100

average in smaller platinum ensembles at the surface, leading to the suppression of reactions requiring more than one platinum atom relative to reactions taking place on single atoms (*7*, *29*).

These smaller ensembles enhance the selectivity for nondestructive reactions. A good example of this effect may be found in the study by den Otter and Dautzenberg (*30*) on hexane reforming at one atmosphere, over platinum and platinum–aluminum on an acidified γ-alumina support. By alloying with aluminum the hydrogenolysis selectivity decreases by a factor of three, whereas the isomerization selectivity increases by a factor of six and the aromatization selectivity by a factor of 1.5.

Our results clearly show that the platinum–iridium reforming catalysts do not belong to the type described above, and for the beneficial action of iridium in platinum another explanation has to be sought. Our AES results show that even at high bulk iridium concentrations the iridium surface concentration is very low. Hence it is to be expected that the behavior of an iridium–platinum reforming catalyst is platinum-like. This is exactly what is found in our heptane reforming experiments (see Fig. 9). It also follows from these experiments that already at a very low iridium atom concentration in the platinum surface the formation of carbonaceous deposits is suppressed, by which the conversion and catalyst stability increases (see Fig. 8). This again is in accordance with our AES results, where it is shown that carbon-covered platinum surfaces are more easily freed from carbon in the presence of iridium.

The mechanism by which the platinum surface is kept clean, as a result of a relatively low surface concentration of iridium sites, is not fully clear. It is likely that carbon atoms, deposited on the platinum, can migrate over a number of platinum sites to the iridium centers in the surface, where they are hydrogenated to methane.

In our experiments an improvement of the selectivity by the presence of iridium, in the direction of more isomerization and aromatization, was not observed (Fig. 9). However, it is to be expected that in industrial reforming, which proceeds at much higher pressures, the suppression of carbon deposition is much more severe than in our one atmosphere experiments. Then the selectivities shift in the direction of more skeletal isomerization and less aromatization and cyclization (see the selectivities found at the start of the running-in period of iridium-poor platinum in Fig. 6, where still little carbon deposition has taken place).

Neither from our experiments nor from the literature is any evidence found for the existence of ordered Pt/Ir phases in small alloy particles or in the catalysts; only monophasic solid solutions are observed. Furthermore, the constancy of the selectivities as a function of the Ir/Pt ratio points to the absence of special ligand effects.

Our experiments are performed at a much lower pressure (10^5 N m^{-2}) and temperature (650 K) than is usual in industrial practice, and the mean diameters of the metal crystallites were about 50 times as high as in the industrial catalysts. Therefore, direct extrapolation of the results to industrial conditions, with respect to conversion and selectivity, is difficult, the more so as in the industrial case promoters are added. In the patents (*2–6*) it is stated that under industrial conditions a high octane C_5^+ reformate is formed for *protracted* on-stream periods without significant yield losses during the course of the reforming operation. This is in good accordance with the general outcome of our work; without any exception the patents claim an improvement of the activity, of the selectivity toward isomerization, and of the stability against coke formation, shown by platinum catalysts on introduction of iridium.

It is interesting to note that Callender and co-workers (*31*) have shown that, with respect to cyclization, the reforming process is not totally bifunctional; cyclization can also proceed on the platinum and acid sites as such. In our experiments, however, the acidic sites were found to be inactive for cyclization, and strong evidence is found that skeletal isomerization over iridum-on-γ-alumina (acidified) is purely bifunctional.

ACKNOWLEDGMENTS

The authors are grateful to Dr. V. Ponec and to Dr. F. J. Kuijers, both of the Gorlaeus Laboratory, University of Leiden, for their stimulating interest and for measuring the Auger spectra. Thanks are also due to Dr. J. A. Don, Delft Technical University, for the determination of the platinum and iridium content of the catalysts by activation analysis, and for helpful discussions. This work was carried out with the financial support of the Netherlands Organization for the Advancement of Pure Research (ZWO), as part of the program of the division "Stichting Scheikundig Onderzoek Nederland."

REFERENCES

1. Jacobson, R. L., Kluksdahl, H. E., McCoy, C. S., and Davis, R. W., *Proc. Am. Pet. Inst.* 1969, 504.
2. U.S. Pat. No. 2,848,377.
3. U.S. Pat. No. 3,839,194.
4. British Pat. No. 1,364,875.
5. U.S. Pat. No. 3,867,280.
6. U.S. Pat. No. 3,953,368.
7. Sachtler, W. M. H., and van Santen, R. A., *in* "Advances in Catalysis" (D. D. Eley, H. Pines, and P. B. Weisz, Eds.), Vol. 26, p. 69. Academic Press, New York, 1977.
8. Raub, E., and Plate, W., *Z. Metallk.* **47**, 686 (1956).
9. Anderson, J. R., and Avery, N. R., *J. Catal.* **5**, 446 (1966).
10. "Selected Values of Chemical Thermodynamic Properties," National Bureau of Standards, Washington, Technical Note 270-4, May 1969.
11. Went, R. C. (Ed.), "Handbook of Chemistry and Physics," 52nd ed. The Chemical Rubber Co., Cleveland, Ohio, 1971.
12. Ciapetta, F. G., and Wallace, D. W., *in* "Catalysis Reviews" (H. Heinemann and J. J. Carberry, Eds.), Vol. 5, p. 67. Marcel Dekker, New York, 1971.
13. Heinemann, H., *in* "Catalysis Reviews-Sci. Eng." (H. Heinemann and J. J. Carberry, Eds.), Vol. 15, p. 53. Marcel Dekker, New York, 1977.
14. Ramaswamy, A. V., Ratnasamy, P., Sivasanker, S., and Léonard, A. J., Proc. Int. Congr. Catal., 6th (London 1976), p. 855. Chemical Society, London, 1977.
15. Tournayan, L., Charcosset, R., and Fréty, R., "Preprints of the fifth Ibero-American Congress on Catalysis," Lisbon, 1976.
16. Gray, T. J., Masse, N. G., and Oswin, H. G., Actes Congr. Int. Catal., 2me (Paris 1960), p. 1697. Edition Technip, Paris, 1961.
17. Bond, G. C., and Webster, D. E., *Plat. Met. Rev.* **10**, 10 (1966).
18. Bond, G. C., and Webster, D. E., *Ann. N.Y. Acad. Sci. U.S.A.* **158**, 540 (1969).
19. Kroptova, N. V., Semenova, A. D., and Vovchenko, G. D., *Russ. J. Phys. Chem.* **49**, 843 (1975).
20. Ramakrishnan, E. S., and Chandrasekharaiah, M. S., *J. Less-Common Met.* **37**, 269 (1974).
21. Kulifay, S. M., *J. Am. Chem. Soc.* **83**, 4916 (1961).
22. de Bruin, M., and Korthoven, P. J. M., *Anal. Chem.* **44**, 2382 (1972).
23. Kuijers, F. J., Thesis, Leiden University, 1978.
24. Gallon, T. E., *Surf. Sci.* **17**, 486 (1969).
25. Brunelle, J. P., Montarnal, R. E., and Sugier, A. A., "Proc. Int. Congr. Catal., 6th (London 1976), Chemical Society, London, 1977.
26. McIntyre, N. S., Vander Auwera-Mahieu, A., and Drowart, J., *Trans. Faraday Soc.* **64**, 3006 (1968).
27. Vander Auwera-Mahieu, and Drowart, J., *J. Chem. Phys. Lett.* **1**, 311 (1967).
28. Weisz, P. B., *in* "Advances in Catalysis" (D. D. Eley, H. Pines, and P. B. Weisz, Eds.), Vol. 13, p. 137. Academic Press, New York, 1962.
29. Hagen, D. L., and Somorjai, C. A., *J. Catal.* **41**, 466 (1976).
30. den Otter, G. J., and Dautzenberg, F. M., *J. Catal.* **53**, 116 (1978).
31. Callender, W. L., Brandenberger, S. G., and Meerbott, W. K., Proc. Int. Congr. Catal., 5th (Florida 1972), Vol. 2, p. 1265. North-Holland Publishing Company, Amsterdam–London, 1973.